An Interferometer for Atoms

David W. Keith, Christopher R. Ekstrom, Quentin A. Turchette, and David E. Pritchard
Massachusetts Institute of Technology, Cambridge, Massachusetts 02139
(Received 7 March 1991)

We have demonstrated an interferometer for atoms. A three-grating geometry is used, in which the interfering beams are distinctly separated in both position and momentum. We used a highly collimated beam of sodium atoms with a de Broglie wavelength of 16 pm and high-quality 0.4-μm-period free-standing gratings which we fabricated using a novel method. The interference signal is 70 counts/s, which allows us to determine the phase to 0.1 rad in 1 min. Applications of atom interferometers are briefly discussed.

PACS numbers: 07.60.Ly, 35.10.−d, 42.10.Jd

There have been several recent proposals for the realization of an atom interferometer,[1] and a number of experiments have demonstrated interference of atoms.[2] In addition to the work reported here, several other groups have recently demonstrated interference fringes for atoms.[3] We report the demonstration of the first interferometer for atoms in the sense that it uses amplitude division to separate the beams in momentum and distinctly separates the beams in space.[4] We note that matter-wave interferometers have been previously demonstrated for electrons and neutrons.[5]

We used a three-grating white-fringe geometry in which the phase of the interference fringes is independent of incident wavelength and angle.[6] Such a geometry allows the largest interference signal for a given beam brightness. Figure 1 shows a schematic of our experiment which we will describe in four parts: the atomic beam system, the gratings, the interferometer system, and the data analysis method.

Our atomic beam system has been considerably improved since it was last described.[7] It is a supersonic nozzle beam of sodium in an argon carrier gas. Adiabatic expansion of the gas after it leaves the nozzle results in a fairly monochromatic beam: $\Delta v/v = 12\%$ with $v = 10^3$ m/s. The sodium has the same velocity as the carrier gas, giving it a de Broglie wavelength of 16 pm. The beam is collimated by two 20-μm slits spaced 0.9 m apart to form a 1-mm×20-μm ribbon-shaped beam with a divergence of 20 μrad. Individual sodium atoms are detected after surface ionization on a 25-μm-diam hot wire (80%-Pt, 20%-Ir alloy) located 1.6 m downstream from the second slit. In order to achieve high ionization efficiency it was necessary to expose the wire to oxygen at regular intervals: 10^{-3} torr O_2 for $\sim$1 min every $\sim$30 min proved to be sufficient. Under these conditions the detector's time response was $\sim$15 ms and the average background was $\sim$20 counts/s. A key problem is that the background signal is dominated by highly non-Poissonian bursts (see example in Fig. 3). Although we cannot directly measure the efficiency, we believe that it is better than 10%. In any case, greater wire efficiency, combined with improvements to our vacuum system and the sodium source, now allows us to achieve detected fluxes of >1 MHz through a 1-mm-high slit. This corresponds to a detected source brightness of 10^{19} $s^{-1}cm^{-2}sr^{-1}$.

The quality of gratings necessary for an interferometer is considerably higher than is needed to demonstrate

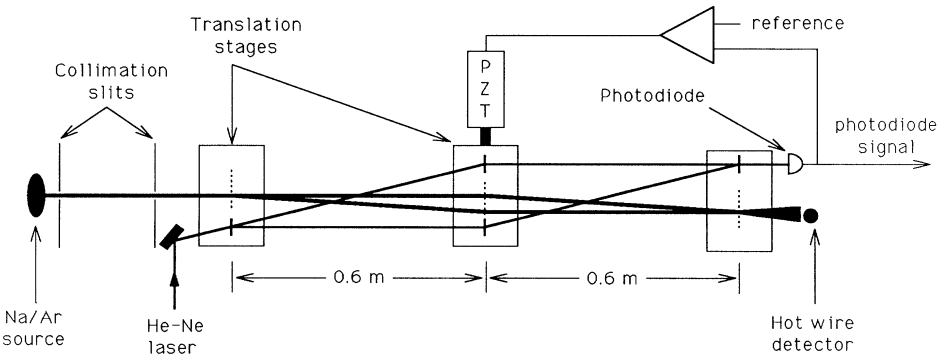

FIG. 1. A schematic of our interferometer showing the active vibration isolation system. Not to scale. The 0.4-μm-period atom gratings are indicated by a vertical dashed line, and the 3.3-μm-period optical gratings by a vertical solid line.

diffraction of atoms. In particular, the gratings must be phase coherent over their entire area. This implies that the grating lines must be straight to the order of their linewidth over the full height of the grating. The transmission of each grating support structure (necessary to achieve the required line straightness) should be high since the final interference signal will be proportional to the third power of this transmission. In addition, the grating line to space ratio must be near 1:1; ideally the grating spaces should be 0.65 period for the first grating and 0.5 for the other two.

Our diffraction gratings consist of arrays of slots in a tensile silicon nitride membrane. Several membranes are formed on a 12×7-mm Si chip. The gratings we used were made in two sizes: 750×40 μm and 500×140 μm with periods of 400 and 200 nm. The grating fabrication process, described briefly below, will be detailed elsewhere.[8] First, a double-polished, ⟨100⟩ Si wafer (250 μm thick) is coated on both sides with 200 nm of low-stress nitride (Si_3N_4) by plasma-enhanced low-pressure chemical vapor deposition. Conventional photolithography is used to pattern the nitride on the back side of the wafer with small rectangles which are aligned with the crystal axis. The Si under these rectangles is etched along the ⟨111⟩ planes using a hot KOH solution, leaving the nitride windows on the front side. The front side of the wafer is then coated with 150 nm of polymethyl methacrylate (PMMA) film and then with 15 nm of Au. Electron-beam lithography is used to expose the grating patterns in the PMMA. We used a JEOL JBX 5DII(U) *e*-beam writer, and took care to minimize the effects of field stitching. The Au is needed to reduce charging of the substrate which can cause writing distortions. The exposed PMMA and the Au are then removed, leaving a direct mask for reactive-ion etching (RIE) of the nitride. It was necessary to develop a highly directional RIE process, which was able to selectively etch nitride using PMMA as a mask. By this method we have made high-quality 200- and 400-nm-period gratings; Fig. 2 shows a completed example.

The interferometer consists of three 400-nm-period gratings mounted 0.663 ± 0.003 m apart on separate translation stages inside the vacuum envelope. During operation, the zeroth- and first-order beams from the first grating strike the middle grating (which is 140 μm wide) where they are diffracted in the first and negative first orders so that they converge at the third grating. At the second (middle) grating the beams have widths of 30 μm (FWHM) and are separated by 27 μm. The first two gratings form an interference pattern in the plane of the third grating, which acts as a mask to sample this pattern. The detector, located 0.30 m beyond the third grating, records the flux transmitted by the third grating.

In order to observe stable fringes, various requirements on mechanical stability and alignment must be met. These requirements are a consequence of the sensitivity of the interferometer to the rotation, acceleration, and translation of the gratings. We now describe these problems, and our solutions to them.

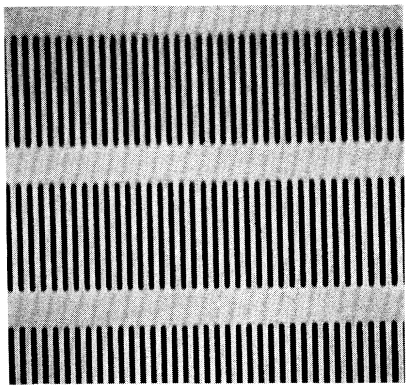

FIG. 2. A scanning electron micrograph of a completed 200-nm-period grating.

The gratings must be aligned with respect to rotations about the beam axis to an angular tolerance given by the beam height over the period (10^{-3} rad). We aligned the gratings by using the 4-μm-period support structures as diffraction gratings for a helium-neon laser. Our grating fabrication method ensures that the support-structure grating is orthogonal to the primary fine-period grating to an accuracy equal to the line straightness of either grating. The primary limitation of this technique is that the grating windows are only 40 μm wide, so that the diffracted laser spots have an angular width of 10^{-2} rad. In practice, we were able to achieve alignment to about 2×10^{-3} rad. The final grating alignment is performed while the experiment is operating, by rotating the middle grating so as to maximize the interferometer fringe contrast.

The interferometer is sensitive to accelerations of the three gratings as a unit. The sensitivity in radians per unit of acceleration is given by $2\pi l^2/v^2 p$, where l is the distance between gratings, v is the atom's velocity, and p is the grating period. In our interferometer this is 13 rad m^{-1}s^2, which can be understood as the phase change due to the translation of the gratings during the atoms 1.3-ms transit through the interferometer. Rotation of the interferometer about the axis perpendicular to its enclosed area causes a phase shift (the Sagnac effect) proportional to the rotational velocity which is given by $4\pi l^2/pv$. In our interferometer this sensitivity is 1.4×10^4 s. Thus, rotation at one Earth rate produces a phase shift of 1 rad. In addition to the phase shifts caused by motion of the three gratings as a unit, the interferometer is sensitive to the relative position of the gratings. In order to observe any fringe contrast, it is necessary that the relative positions of the three gratings be stationary to within $\sim \frac{1}{4}$ period (100 nm) during the time the final grating samples the fringe pattern.

We have solved these problems using a combination of

passive isolation and active feedback. The passive isolation system consists of small rubber feet which support the apparatus. This simple isolation system reduced the rms motion, due mainly to building noise, by an order of magnitude to ~ 0.5 μm. It is difficult to improve this further by using more sophisticated pneumatic supports because such systems have unacceptably high levels of low-frequency rotational noise. The active feedback system uses a laser interferometer which has the same transmission grating geometry as the atom interferometer. The 3.3-μm-period gratings for the optical interferometer are mounted on the same three translation stages as the matter-wave gratings in order to record the relative alignment of the matter-wave interferometer. The error signal from the optical interferometer measures the relative alignment of the three grating platforms; it is applied to a piezoelectric translator (PZT) through a feedback network in order to stabilize the platforms. Using this system we have reduced the relative rms motion of the gratings from ~ 500 to 40 nm. The active feedback system is used to stabilize the relative positions of the three gratings at frequencies below ~ 100 Hz. This system works best at low frequencies (< 10 Hz) where the passive system is least effective. The reduction of relative motion provided by the active system allows us to use long integration times when we are looking for the interference signal.

The data necessary to determine the interferometer phase and fringe contrast are acquired as follows. A triangle wave at ~ 0.2 Hz is applied to the reference port of the optical-interferometer feedback network with the amplitude of the reference wave chosen so that the optical interferometer is driven through $\frac{1}{3}$ of an optical fringe. The raw signal from the optical interferometer is then recorded simultaneously with the signal from the atom counting electronics. Both signals are sampled at 10-ms intervals for a total time of ~ 2 min.

The data are then analyzed by first calculating the optical interferometer's relative position from the measured intensity, the optical fringe limits, and the known 3.3-μm period of the gratings. Figure 3 shows an example of these data. Next, the data obscured by noise spikes from the hot wire are discarded (typically about 2% of the total samples). This is done automatically, without reference to the position information. Finally, the atom count data are summed into bins according to the position at which they were taken and the result is then divided by the time spent taking samples at that position. Figure 4 shows the measured interference signal.

We have performed extensive numerical simulations of this experiment. The simulations were two dimensional with a transverse resolution of 1 nm, and included an incoherent sum over source points with the experimentally measured velocity distribution. The calculated contrast in this configuration is 25%; our measured contrast is 13%. We ascribe the discrepancy to a number of small effects including grating imperfections and creep in the alignment PZT.

The peak-to-peak amplitude of our interference signal is 70 counts/s, which enables us to determine the interferometer phase to a precision of 0.1 rad in 1 min. The large low-frequency gain of our position stabilization system provides measured atom-interferometer phase drift of less than 0.1 rad over 10 min.

In the near future we plan to insert a septum between the beams of our interferometer. If needed, we can increase the beam separation by using 0.2-μm-period gratings and by using xenon as a carrier gas in our source. We should then be able to make accurate measurements of the Aharonov-Casher[9] phase and the polarizability of sodium.

Atom interferometers may also be used for tests of

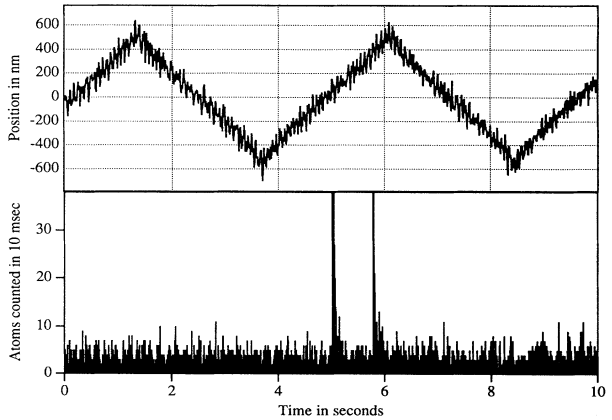

FIG. 3. 10 s of raw data. The upper graph shows the relative transverse position of the interferometer gratings as measured by the optical interferometer. The lower graph shows the number of atoms per 10-ms bin. Peak heights of the off-scale hot-wire noise bursts are 92 and 304 counts, respectively.

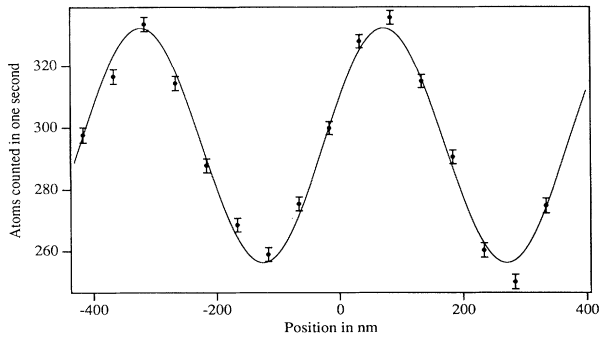

FIG. 4. Interference signal from 400 s of data (~ 23 s per point). Background hot-wire noise of 40 counts/s subtracted. The solid line is a least-squares fit by a sine function with 400-nm period. Error bars are 1 standard deviation assuming Poissonian noise, and slightly underestimate the noise because of the super-Poissonian character of the hot-wire background.

basic quantum mechanics and perhaps for tests of general relativity.[10]

We would like to thank Mike Rooks and other staff at the National Nanofabrication Facility. Bruce Oldaker and Garth Zeglin provided valuable technical assistance during the early phases of this work. We gratefully acknowledge funding from ONR Contract No. N0014-89-J-1207, ARO Contract No. DAAL03-89-K-0082, and Joint Services Electronics Program Contract No. DAAL03-89-C-0001.

[1]S. Altshuler and L. M. Frantz, U. S. Patent No. 3,761,721 (1973); V. P. Chebotayev *et al.*, J. Opt. Soc. Am. B **2**, 1791 (1987); D. W. Keith and D. E. Pritchard, in *New Frontiers in QED and Quantumoptics,* edited by A. O. Barut (Plenum, New York, 1990); Ch. J. Borde, Phys. Lett. A **140**, 10 (1989).

[2]I. Estermann and O. Stern, Z. Phys. **61**, 95 (1930); D. W. Keith, M. L. Shattenburg, H. I. Smith, and D. E. Pritchard, Phys. Rev. Lett. **61**, 1580 (1988); A. Faulstich, O. Carnal, and J. Mlynek, in Proceedings of the International Workshop on Light Induced Kinetic Effects, Elba, Italy, 1990, edited by L. Moi *et al.* (to be published).

[3]O. Carnal and J. Mlynek, preceding Letter, Phys. Rev. Lett. **66**, 2689 (1991); F. Riehle *et al.* (to be published); S. Chu (private communication).

[4]Devices such as the one presented here in which wave fronts are divided (using either wave-front or amplitude division), spatially separated, and purposefully recombined (e.g., using reflection or refraction) are universally referred to as interferometers. When all of these conditions are not met, there is a division of opinion. In particular, Young's experiment is not generally classed as an interferometer [e.g., M. Born and E. Wolf, *Principals of Optics* (Pergamon, New York, 1980), 6th ed., Chap. VII].

[5]Neutrons: H. Maier-Leibnitz and T. Springer, Z. Phys. **167**, 368 (1962); The first "perfect-crystal" neutron interferometer reported was by H. Rauch, W. Treimer, and U. Bonse, Phys. Lett. **47A**, 369 (1974); electrons: L. Marton, J. Arol Simson, and J. A. Suddeth, Phys. Rev. **90**, 490 (1954).

[6]B. J. Chang, R. Alferness, and E. N. Leith, Appl. Opt. **14**, 1592 (1975). Our geometry is identical to that used in a three-diffraction-grating interferometer for neutrons: M. Gruber, K. Eder, A. Zeilinger, R. Gahler, and W. Mampe, Phys. Lett. A **140**, 363 (1989).

[7]P. L. Gould, Ph.D. thesis, MIT (unpublished); D. W. Keith, M. L. Shattenburg, H. I. Smith, and D. E. Pritchard, Phys. Rev. Lett. **61**, 1580 (1988); most recently in D. W. Keith, Ph.D. thesis, MIT (unpublished).

[8]D. W. Keith and M. J. Rooks (to be published).

[9]Y. Aharonov and A. Casher, Phys. Rev. Lett. **53**, 319 (1984).

[10]L. E. Stodolsky, Gen. Relativ. Gravitation **11**, 391 (1979).

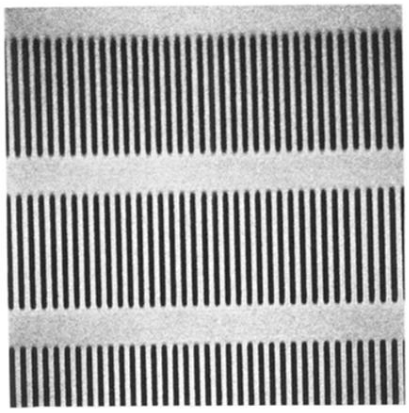

FIG. 2. A scanning electron micrograph of a completed 200-nm-period grating.